



## RESEARCH ARTICLE

# Effects of climate change on major elements of the hydrological cycle in Aksu River basin, northwest China

Peng Yang<sup>1</sup>  | Wenyu Wang<sup>1</sup> | Jun Xia<sup>2,3</sup> | Yaning Chen<sup>4</sup> |  
Chesheng Zhan<sup>3</sup> | Shengqing Zhang<sup>1</sup> | Cai Wei<sup>1</sup>  | Xiangang Luo<sup>1</sup> | Jiang Li<sup>5</sup>

<sup>1</sup>School of Geography and Information Engineering, China University of Geosciences, Wuhan, China

<sup>2</sup>State Key Laboratory of Water Resources and Hydropower Engineering Sciences, Wuhan University, Wuhan, China

<sup>3</sup>Key Laboratory of Water Cycle and Related Land Surface Processes, Institute of Geographic Sciences and Natural Resources Research, Chinese Academy of Sciences, Beijing, China

<sup>4</sup>State Key Laboratory of Desert and Oasis Ecology, Xinjiang Institute of Ecology and Geography, Chinese Academy of Sciences, Urumqi, China

<sup>5</sup>Information Center, Department Natural Resources of Hubei Province, Wuhan, China

## Correspondence

Peng Yang, School of Geography and Information Engineering, China University of Geosciences, Wuhan 430074, China.

Email: [yangpenghb@foxmail.com](mailto:yangpenghb@foxmail.com)

Jun Xia, State Key Laboratory of Water Resources and Hydropower Engineering Sciences, Wuhan University, Wuhan.

Email: [xiaj@igsnr.ac.cn](mailto:xiaj@igsnr.ac.cn)

Yaning Chen, State Key Laboratory of Desert and Oasis Ecology, Xinjiang Institute of Ecology and Geography, Chinese Academy of Sciences, Urumqi.

Email: [chenyn@ms.xjb.ac.cn](mailto:chenyn@ms.xjb.ac.cn)

## Funding information

Strategic Priority Research Program of the Chinese Academy of Sciences, Grant/Award Number: XDA23040504; Youth Fund for Humanities and Social Science Research of the Ministry of Education, Grant/Award Number: 20YJCZH207

## Abstract

Water resources systems in arid regions are sensitive to climate change, which critically impacts the water cycle. In this study, we applied historical hydrometeorological data, CMIP5 data, and a large-scale hydrological model (Community Land Model–Distributed Time-Variant Gain Model [CLM–DTVGM]) to study the impact of climate change on the hydrological cycle (i.e., runoff, actual evapotranspiration ( $ET_a$ ), and terrestrial water storage [TWS]) under different scenarios at the Aksu River basin (ARB) located in the arid region of northwest China. The primary findings of this study: (a) As the determination coefficient ( $R^2$ ) and Nash–Sutcliffe efficiency coefficient (NSE) reached desirable levels ( $R^2 \geq 0.583$ ,  $NSE \geq 0.371$ , and root-mean-square error  $\leq 155.727$ ), the CLM–DTVGM achieved a better simulation of runoff in the ARB; under climate change, the runoff depth in the irrigation area became shallower and followed a decreasing trend, with a minimum depth of 0.5 mm and a significant decreasing trend of  $-8 \text{ mm}\cdot\text{a}^{-1}$ . (b) Along with changes in the precipitation and temperature of the baseline period (i.e., 1980–2010), runoff,  $ET_a$ , and TWS were predicted to change significantly in future scenarios. (c) Climate change significantly impacted the historical runoff from the Shaliguilanke and Xiehela hydrological stations, with correlation coefficients larger than 0.9; however, the runoff from the Alaer hydrological station was not affected. However, runoff,  $ET_a$ , and TWS in the ARB were very closely correlated with climate change in the future scenarios, with correlation coefficients exceeding 0.9. Related research in the future would be important for guiding the sustainable development of the ARB.

## KEYWORDS

climate change, CLM–DTVGM, CMIP5, hydrological cycle

## 1 | INTRODUCTION

Climate change leads to the occurrence of extreme climate events that have a fatal impact on humans and the ecological system, and it is currently a major concern of scholars and politicians (Gudmundsson *et al.*, 2021; Mengistu *et al.*, 2021; Pokhrel *et al.*, 2021). As an important medium for heat and material exchange on Earth, water resources are significantly affected by climate change (Liu and Woo, ; Mastrotheodoros *et al.*, 2020; Pokhrel *et al.*, 2021). The effects of climate change on water resources systems are usually expressed through the effects of hydrological variables (e.g., precipitation and temperature) on the hydrological cycle (Huntington, 2006). The characteristics of the hydrological cycle and its associated extreme hydrological events, such as floods and droughts, are closely related to climate change, resulting in the loss of life and property (Gudmundsson *et al.*, 2021; Pokhrel *et al.*, 2021). The area and number of regions affected by these extreme hydrological events are growing (Conway and Schipper, 2011; Yang *et al.*, 2019b). In particular, regions and watersheds recharged by snow and ice melt are heavily affected by climate change (Xu *et al.*, 2011; Qin *et al.*, 2020). Therefore, although there is a wealth of relevant research results, the impact of climate change on different hydrological cycles still needs to be elucidated. It is very important for understanding the mechanism of climate change impact on water resources, the change pattern of water resources system and the formulation of risk-averse policies (Meaurio *et al.*, 2017; Zhao *et al.*, 2019; Hu *et al.*, 2021).

The Aksu River (AR) originates from the middle of the Tianshan Mountains and is the major water source of the Tarim River basin (TRB) (Xu *et al.*, 2011; Fan *et al.*, 2014). In addition, the AR feeds a vast and well-developed irrigated agriculture in the Aksu River basin (ARB) (Chen *et al.*, 2016a). The ARB also plays an essential role in the economy and human health in the TRB (Chen *et al.*, 2016a). Because of the high altitude of its source area, the meltwater from snow-ice and glaciers is the dominant source of runoff in the ARB, accounting for more than 50% of the total runoff (Zhang *et al.*, 2019). However, the ARB has witnessed a large rise in runoff and an ice loss in glaciers during the last 50 years due to climate change (Tao *et al.*, 2011; Xu *et al.*, 2011; Zhang *et al.*, 2019). Furthermore, the ARB ecosystem is fragile; thus, the occurrence of extreme hydrological cycle events, especially droughts, significantly impacts the ecological security of the basin (Wang *et al.*, 2014; Chen *et al.*, 2016a; Wang *et al.*, 2018). However, it must be determined how climate change has already affected the hydrologic cycle in the ARB and how it will affect it in the future.

Several studies have elucidated the effects of climate change on the hydrological cycle in the ARB, owing to its special geographical location and its ecological and economic

importance in the Tarim Basin. The results of these studies are almost unanimous, revealing a sharp decrease in snow-ice resources and a temporary sharp increase in runoff (Xu *et al.*, 2011; Fan *et al.*, 2014; Wang *et al.*, 2014; Wang *et al.*, 2018; Zhang *et al.*, 2019). Therefore, many experts have pointed out that the teleconnection index significantly influences the changes in runoff in the ARB (Wang *et al.*, 2014; Yao *et al.*, 2020). Fan *et al.* (2014) pointed out the direct effects of precipitation and temperature on runoff in the ARB in the past 50 years based on correlation and partial correlation. Deng *et al.* (2019) reported the impacts of glacier and snow variations on regional runoff in the ARB. However, they neglected the coupling effect of temperature and precipitation on runoff and other factors of the hydrological cycle. Further, the authors did not explain how changes in precipitation and temperature affect hydrological processes from the perspective of hydrological mechanisms, or how precipitation and temperature will respond to hydrological processes in future scenarios.

Currently, the proposal and development of global climate models (GCMs) provide important technical tools and data products for studying global climate change, especially under future scenarios (Chen *et al.*, 2020; Dai *et al.*, 2020; Homsí, 2020). For numerous GCMs (e.g., BCC\_CSM1.1, BCC-CSM1.1-M, and BNU-ESM), different models with varying spatiotemporal resolutions have been devised by different countries or organizations; however, they have all been proposed based on the framework of future emission scenarios (Dai *et al.*, 2020; Yin *et al.*, 2021). Furthermore, prior research has revealed that various GCMs correspond to distinct biases and that GCMs used in regional-scale studies must be downscaled (Homsí, 2020; Mengistu *et al.*, 2021). However, the selection of GCMs has often been neglected; previous studies have used as many GCMs as possible, which inevitably leads to the distortion of information on the study subjects (Zhang *et al.*, 2015).

Therefore, to study the impact of climate change on the hydrological cycle, we attempted to (a) drive a large-scale hydrological model analysis and discuss the applicability of the model in the ARB, (b) analyse the characteristics of changes in the major hydrological cycle elements of the ARB under climate change, and (c) explore the relationship between the coupling effect of precipitation and temperature and the major hydrological cycle elements under historical and future scenarios (i.e., RCP2.6, RCP4.5, and RCP8.5).

## 2 | STUDY AREA

The AR originates in Kyrgyzstan and crosses the south side of the Tianshan Mountains before draining into the Tarim River (TR) in China (Figure 1) (Chen *et al.*, 2009; 2014; 2016a). Because of the influence of the high altitude and snow, the

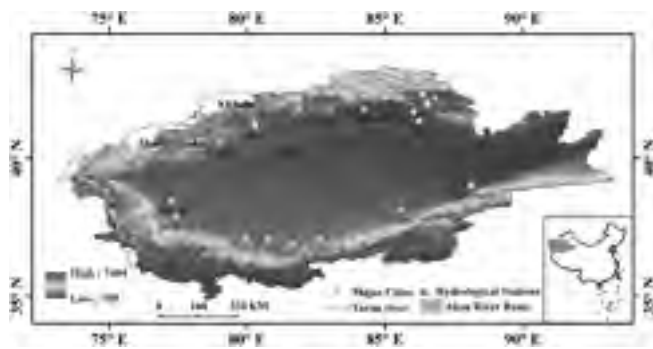


FIGURE 1 Study area and its location in China (see also in Yang *et al.*, 2021)

primary water supply of the ARB is snow meltwater, which provides 73.2% of the water (approximately  $80.6 \times 10^8 \text{ m}^3 \cdot \text{a}^{-1}$ ) among the three major headstreams (i.e., AR, Yarkant River, and Hotan River) for the mainstream of the TR, thereby supporting human activities and the environment in the middle and lower reaches of the TRB (Chen *et al.*, 2009; Yang *et al.*, 2021). The ARB experiences low precipitation, high evaporation, and frequent drought episodes in a typical temperate continental climate (Yang and Chen, 2015; Chen *et al.*, 2016a; 2016b; Yang *et al.*, 2017). Both temperature and snowmelt have increased since the 1970s because of climate change, resulting in aggravated wetting events and changes in the water cycle (Yang and Chen, 2015).

Irrigation agriculture is the agricultural development style used in the ARB, in which crop growth is mostly dependent on the irrigation of rivers and reservoirs in the basin (Huang *et al.*, 2015; Yang *et al.*, 2018a). Meanwhile, the population and cultivated land area of the basin have grown substantially along with the growth of the social economy, which has increased irrigation water demand and water consumption for economic activities across the basin (Chen *et al.*, 2009; Huang *et al.*, 2015; Yang *et al.*, 2019a). Simultaneously, key challenges in the ARB include a limited water supply, chaotic development of water resources, polluted river water due to irrigation, and strain on ecological water resources caused by vegetable production (Chen *et al.*, 2009; 2016b) (Figure 1).

## 3 | DATA AND METHODS

### 3.1 | Data

#### 3.1.1 | Historical hydrometeorological data

The monthly runoff data of three hydrological stations (i.e., Shaliguilanke, Xiehela, and Alaer) in the ARB from 1980 to 2010 were derived from the hydrological yearbook of the People's Republic of China. Runoff from the

Shaliguilanke and Xiehela hydrological stations was chosen as a mountain water resource for agricultural operations, whereas runoff from the Alaer hydrological station was chosen as an ecological water supplement for the mid- to downstream area of the TR.

In addition, precipitation, average temperature, maximum temperature, minimum temperature, sunshine hours, wind speed, relative humidity, and average air pressure among the daily meteorological data from 01/01/1960 to 12/31/2010, which were sourced from the national meteorological data sharing service network (available at <http://www.cma.gov.cn>), have been used to drive the hydrological model.

#### 3.1.2 | Basic geographic data

Digital elevation data with a spatial resolution of 90 m were obtained from the Shuttle Radar Topography Mission (<http://srtm.csi.cgiar.org/>) and resampled to 1 km for model driving. Land use data with a spatial resolution of 1 km were downloaded from the Resource and Environment Data Center, Chinese Academy of Sciences (<http://www.resdc.cn/>). The soil database with a spatial resolution of 1 km was obtained from the Environmental and Ecological Science Data Center for West China, National Natural Science (<http://westdc.westgis.ac.cn/>). The Ministry of Water Resources of the People's Republic of China provided border information for the basin.

#### 3.1.3 | Global climate model data

Coupled Model Intercomparison Project Phase 5 (CMIP5) provided multiple models for assessing the mechanisms coupled with the carbon cycle and clouds, examining climate prediction, and understanding the cause of a range of responses from similar models (Mcsweney *et al.*, 2015; Zhang *et al.*, 2015; Bronselaer *et al.*, 2018). CMIP5 is meant to provide a framework for coordinated climate change experiments, and it has contributed generously to projects predicting future climate change (Wang, 2012; Yang *et al.*, 2019b; Tian and Dong, 2020). The representative concentration pathways (RCPs) database is a concise dataset that includes long-term historical climate simulations and future climate change prediction data worldwide (e.g., RCP2.6, RCP4.5, and RCP8.5) (Chang *et al.*, 2012; Koven *et al.*, 2013; Yang *et al.*, 2019b). In this study, we employed six GCMs (i.e., BCC\_CSM1.1, BCC-CSM1.1-M, BNU-ESM, FGOALS-g2, FGOALS-s2, and FIO-ESM), whose accuracy has been frequently proven. We down-scaled these data using statistical approaches before driving the hydrological model at the basin scale in the ARB.

## 3.2 | Methods

### 3.2.1 | Community Land Model–Distributed Time-Variant Gain Model

The large-scale hydrological model CLM–DTVGM is a coupling of the Community Land Model (CLM) 3.5 and Distributed Time-Variant Gain Model (DTVGM) (Yang *et al.*, 2019a). The Institute of Atmospheric Physics has developed CLM 3.5, in which the land and land surface models are from the Chinese Academy of Sciences and the National Center for Atmospheric Research, respectively (Niu and Yang, 2006; Thornton and Zimmermann, 2007; Yang *et al.*, 2019a). CLM 3.5 has two improvements (i.e., new surface datasets and a new set of parameterizations) compared with CLM 3.0. DTVGM, as proposed by Xia (2002) based on nonlinear theory. The model can extract watershed boundary and sub-basin information based on geographic information system technology and digital elevation models. Also, it has been widely and successfully applied to many regions and watersheds globally (Song *et al.*, 2011; Yang *et al.*, 2019a).

The CLM–DTVGM couples the advantages of CLM for simulation on large-scale watersheds with the advantages of the DTVGM nonlinear theory for the accurate and concise simulation of the effects of human activities on runoff (Zhan *et al.*, 2013; Yang *et al.*, 2019a). Specifically, the time-varying gain factor and the convergence mechanism of wave motion in the DTVGM model replace the first-order linear equations in the flow and convergence module of CLM 3.5, allowing the accurate simulation of two-dimensional hydrological processes and of the impact of human activities on hydrological processes (Zhan *et al.*, 2013; Xia *et al.*, 2016; Yang *et al.*, 2019a). In this study, the uncertainty analysis of the parameters in the DTVGM model was implemented based on the PSUADE platform and the SCE-UA method (Li *et al.*, 2009).

### 3.2.2 | Downscaling method of global climate model

In this study, the scoring method proposed by Fu *et al.* (2013) was applied to the selection of GCMs in the ARB. Models with low scores were excluded from the set of alternative GCMs, whereas models with higher scores were applied in the downscaled calculation and CLM–DTVGM driving. The scoring and downscaling methods can be expressed by Equations (1) and (2),

$$S = \sum_{i=1}^n \left( \omega_i \times \frac{x_{i,j} - x_{i,\min}}{x_{i,\max} - x_{i,\min}} \times 6 \right), \quad (1)$$

where  $x_{i,j}$  represents the relative error of the output of the  $j$ th GCM and the  $i$ th observation evaluated index;  $x_{i,\min}$  and  $x_{i,\max}$  stand for the minimum and maximum values of the  $i$ th index in the alternative GCMs, respectively;  $\omega_i$  is the weight of the  $i$ th index;  $i$  and  $j$  indicate the order numbers of the evaluated index and GCMs, respectively; and  $n$  stands for the number of evaluated indices.

The details of the downscaling method with simple and quick features are as follows (Zhang *et al.*, 2015; Yang *et al.*, 2019a),

$$\begin{cases} P_{F,i} = \left( \frac{P_{f,i}}{P_{h,i}} - 1 \right) \times 100\%, \\ T_{F,i} = T_{f,i} - T_{h,i} \end{cases}, \quad (2)$$

where  $P_{F,i}$  and  $T_{F,i}$  are the adjustment coefficients for precipitation and temperature in the  $i$ th month, respectively;  $P_{f,i}$  and  $T_{f,i}$  represent the average precipitation and temperature in the  $i$ th month in the future, respectively; and  $P_{h,i}$  and  $T_{h,i}$  denote the average precipitation and temperature in the  $i$ th month in history, respectively. Historical data after downscaling are compared with measured historical data based on correlation coefficients. In this study, 2010–2100 was regarded as the future period and 1980–2010 as the historical. In order to analyse the characteristics of climate change in different future periods, we have divided them into immediate term (i.e., 2010–2039), medium term (i.e., 2040–2069) and long term (i.e., 2070–2099).

### 3.2.3 | Multiple wavelet coherence

Multiple wavelet coherence (MWC) is a special case that extends from bivariate to multivariate. Therefore, it is necessary to consider the correlation between variables when calculating the coherence and phase difference (Hu and Si, 2016; Su *et al.*, 2019). In general, the squared multiple wavelet coherence between series  $X_1$  and all other series  $X_2, \dots, X_p$  is defined as

$$R_{1(2,3,\dots,p)}^2 = R_{1(q)}^2 = 1 - \frac{M^d}{S_{11}M_{11}^d}, \quad (3)$$

where  $M$  is the  $p \times p$  matrix of smoothed cross-wavelet spectra of  $S_{ij}$ , which can be expressed as

$$S_{ij} = S(W_{xi,xj}) \left( S_{ij} = S_{ji}^*, S_{ij} = S(|W_{xi}|^2) \right), \quad (4)$$

$$M = \begin{bmatrix} S_{11} & \cdots & S_{1p} \\ \vdots & \ddots & \vdots \\ S_{p1} & \cdots & S_{pp} \end{bmatrix}. \quad (5)$$



$M_{ij}^d$  is the cofactor of element  $(i; j)$  of  $M$ , which can be calculated as

$$M_{ij}^d = (-1)^{i+j} \det(M_i^j), \quad (6)$$

where  $M_i^j$  denotes the submatrix from  $M$  by removing the  $i$ th row and  $j$ th column. The partial wavelet coherency of  $X_1$  and  $X_j$  ( $2 \leq j \leq p$ ) is given by

$$\rho_{1j,qj} = - \frac{M_{j1}^d}{\sqrt{M_{11}^d M_{jj}^d}}, \quad (7)$$

where  $q_j = \{2, \dots, p\}$ . The partial wavelet coherency of  $X_1$  and  $X_j$  ( $2 \leq j \leq p$ ) can be obtained from

$$r_{1j,qj} = - \frac{M_{j1}^d}{\sqrt{M_{11}^d M_{jj}^d}}. \quad (8)$$

For the MWC, the 95% significance level was calculated based on the Monte Carlo method (Grinsted *et al.*, 2004; Hu and Si, 2016).

## 4 | RESULTS

### 4.1 | Historical and future hydrological processes in the Aksu River basin

In this study, three representative hydrological stations were selected to evaluate the CLM-DTVGM (Figure 2).

Based on the evaluation index, we found that the simulation effect of the Alaer hydrological station was superior to those of the Shaliguilanke and Xiehela hydrological stations. Moreover, the mean value of the determination correlation coefficient ( $R^2$ ) in the calibration period was greater than 0.75, whereas that of the NSE was greater than 0.71. In comparison, both the average values of  $R^2$  and NSE in the validation period were lower than those in the calibration period. Although there is a poor simulation effect in the flood season, the CLM-DTVGM may better describe the runoff process in the ARB. Similar results in the northwest arid region of China were also reported by Xia *et al.* (2016).

To drive the large-scale hydrological model CLM-DTVGM, the future scenario data from CMIP5 during 2010–2100 must be downscaled, as shown in Figure 3. From the spatial distribution of downscaled annual precipitation and temperature, the precipitation in the west of the ARB was found to be higher than that in the east in the future scenarios (Figure 3a,d,g); conversely, the temperature in the west was lower than that in the east (Figure 3b,e,h). However, the precipitation fluctuated frequently under the three scenarios (i.e., RCP2.6, RCP4.5, and RCP8.5), and the precipitation and temperature in the ARB were predicted to gradually increase in the future (Figure 3c,f,l).

Figure 4 describes the Mann–Kendall test for the annual runoff depth in the ARB in future scenarios. The spatial distribution of the annual runoff depth in the future was relatively consistent during 2010–2100, with a smaller runoff depth in the irrigation area and a larger

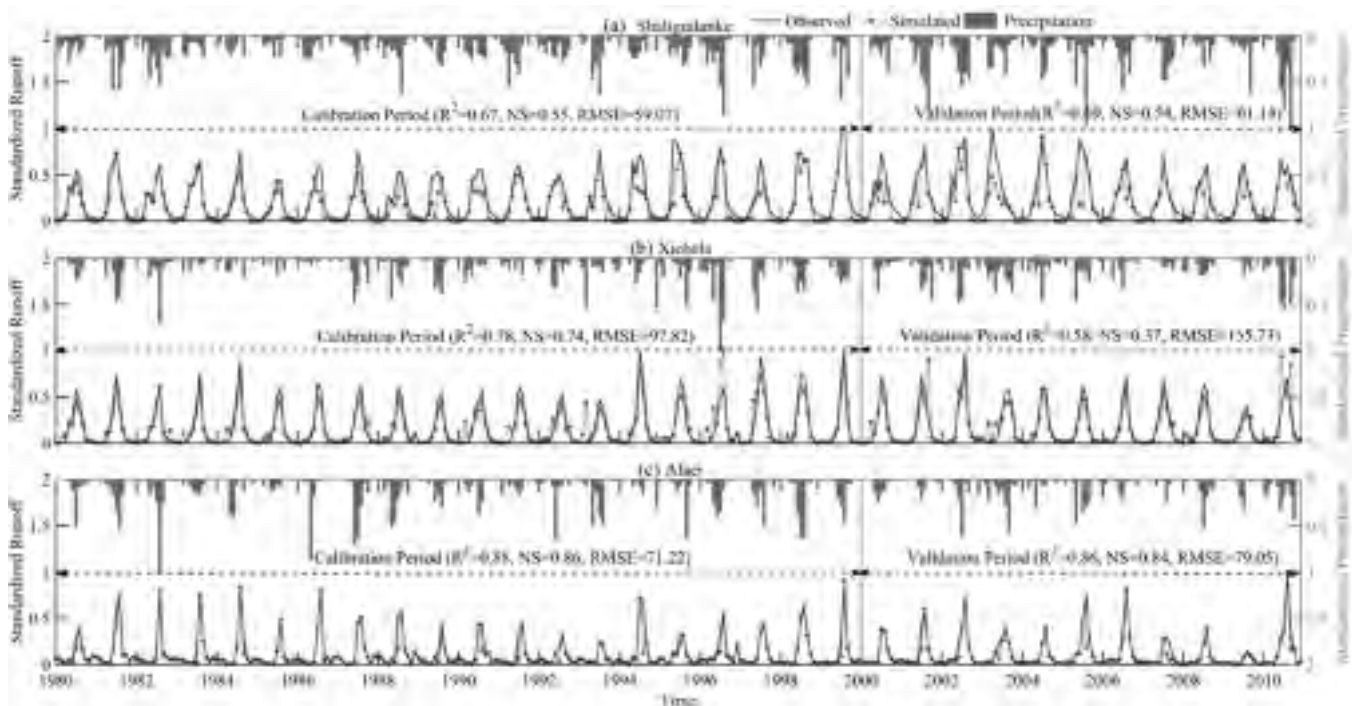


FIGURE 2 Hydrological process simulation of major hydrological stations in the Aksu River basin (see also in Yang *et al.*, 2021)

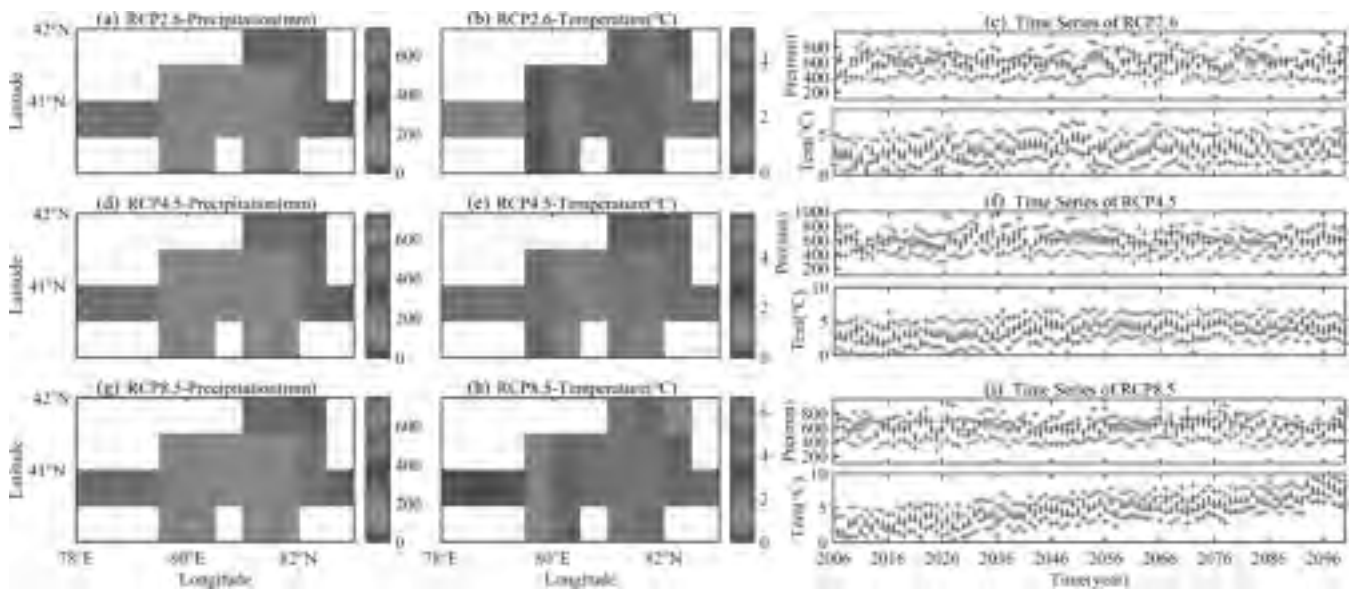


FIGURE 3 Temporal and spatial distribution of future major meteorological factors (i.e., P and T) in the Aksu River basin under climate change (the red stars in (c, f, i) represent the extremes of P and T on the spatial domain in a specific year, and the box plots represent the quartiles of P and T on the spatial domain in a specific year)

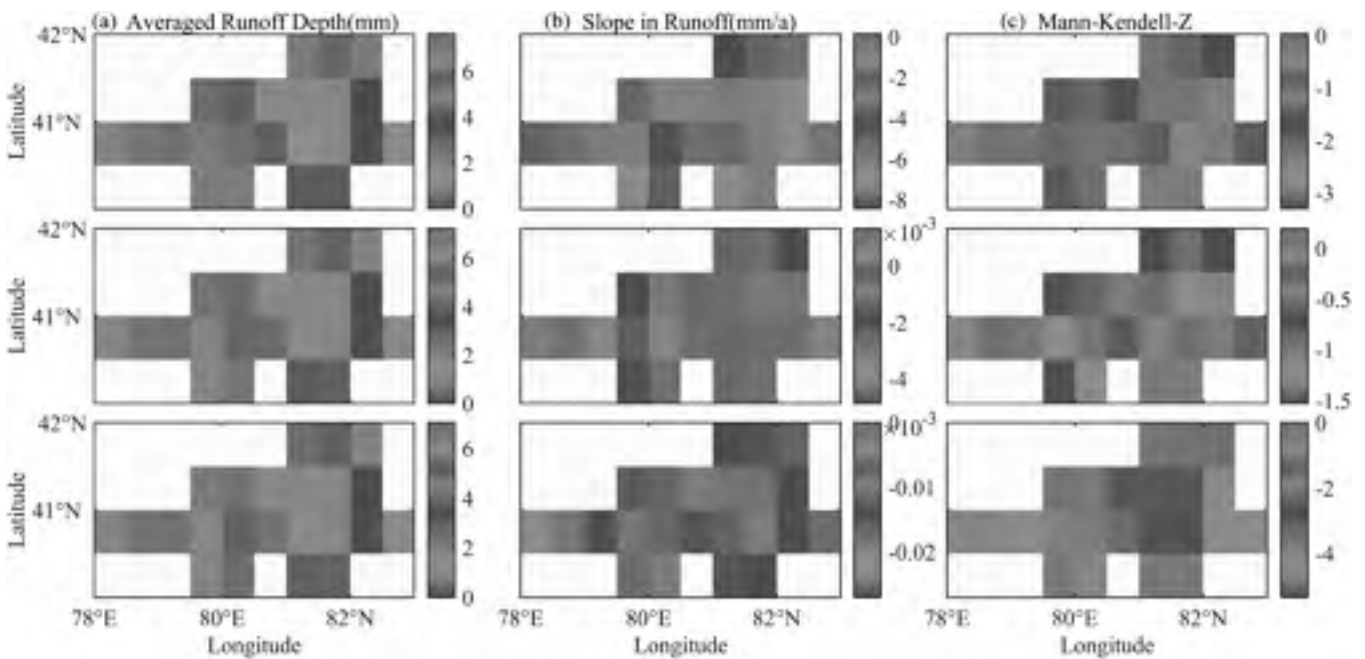


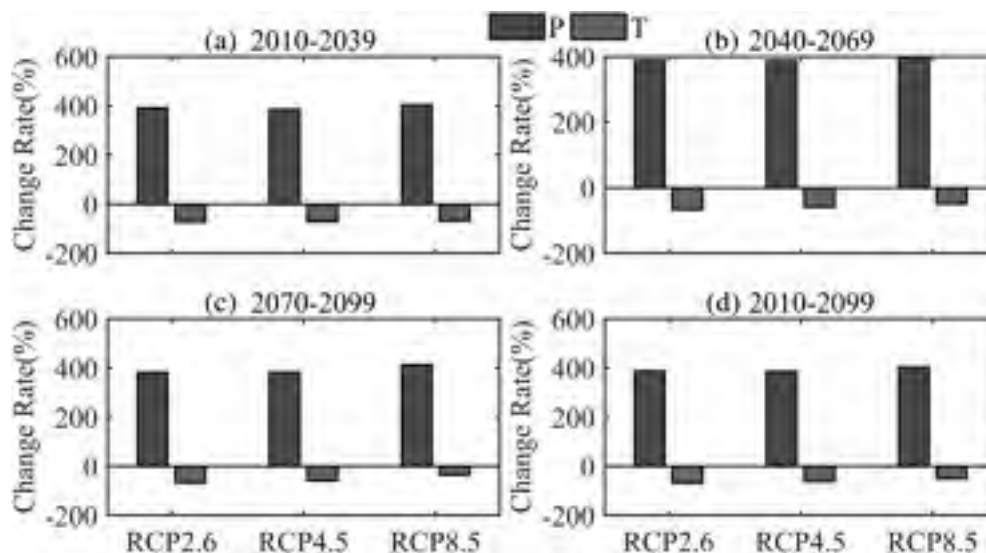
FIGURE 4 Temporal and spatial changes in future runoff in the Aksu River basin under climate change

runoff depth in the mountain outlet. In addition, it showed a decreasing trend from 2010 to 2100, with a larger decrease rate in the west of the basin. Furthermore, except for the nonsignificant decrease under RCP4.5, the decreasing trend of runoff depth in the east-central part of the ARB under RCP2.6 and in the entire ARB under RCP8.5 reached significant levels ( $p < .05$ ).

## 4.2 | Changes in major hydro-meteorological elements in the Aksu River basin relative to those in historical periods

Figure 5 shows the changes in precipitation and temperature in the ARB during different periods (i.e., 2010–2039, 2040–2069, 2070–2099, and 2010–2100) relative to the

**FIGURE 5** Future precipitation and temperature changes relative to historical precipitation and temperature in the Aksu River basin



baseline period (1980–2009). Precipitation was found to increase significantly in different periods in the future; however, the temperature was found to decrease significantly. Precipitation would increase more in different periods in the future, with a maximum increase of 400% during 2010–2039 and 2040–2069 under RCP8.5. In contrast, the decline of temperatures varied over the historical periods across future periods and scenarios, with a maximum cooling of 50%. This result did not corroborate those of previous studies, which may be because of errors in the interpolation results due to the limited number of observation sites or because the baseline period in this study was different from those of the other studies.

To analyse the impact of climate change on the main hydrological elements (i.e., actual evapotranspiration ( $ET_a$ ), runoff, and terrestrial water storage (TWS), which is the sum of unsaturated soil water and groundwater), we also analysed the intra-annual distribution of the main meteorological elements (i.e., precipitation and temperature) and the major hydrological elements derived from CLM-DTVGM (Figures 6–8). Figure 6 shows the intra-annual distribution of historical and future precipitation, temperature, and  $ET_a$  in the ARB. The historical peak of precipitation occurred in July, whereas that of future precipitation occurred in May. In comparison, the intra-annual distribution of historical precipitation was relatively flat, with maximum monthly precipitation as much as 100 mm in RCP2.6 and RCP4.5, as well as maximum precipitation of 110 mm in RCP8.5; however, the intra-annual distribution of future precipitation showed larger fluctuations. In addition, precipitation was significant in autumn. There was a significant intra-annual variation in future  $ET_a$ , and the peak of  $ET_a$ , at almost 95 mm, occurred 2 months after the peak of precipitation. Moreover, the maximum  $ET_a$  was almost synchronized with the

maximum temperature, while the  $ET_a$  during 2070–2099 in RCP8.5 was significantly larger than those in the other periods and scenarios.

Figure 7 shows the relationship between the intra-annual monthly precipitation, temperature, and runoff. The intra-annual peak of runoff in the future scenarios occurred in March, and the intra-annual peak of precipitation occurred 2 months later than the peak of runoff; however, the intra-annual extreme low values of future runoff and precipitation were more synchronized (Figure 7a–c). The maximum runoff for the period 2010–2039 under the three future scenarios occurred in March, at a runoff depth of approximately 100 mm. The intra-annual maximum runoff occurred 3 months before the intra-annual maximum temperature (Figure 7d–f).

Figure 8 shows the relationship between the intra-annual precipitation, temperature, and TWS. There was a significant seasonal variation in the future intra-annual TWS and precipitation, with the annual TWS maximum occurring in June and that of precipitation occurring 1 month later. In addition, TWS was decreasing in different periods, with the highest TWS occurring in 2010–2039, followed by those in 2040–2069 and 2070–2099. The lowest value of future TWS occurred in November, and an increasing trend in the different periods followed (Figure 8a–c). However, a comparative study indicated that the extreme values of intra-annual TWS occurred 1 month earlier than the extreme values of intra-annual temperature in the future scenarios (Figure 8d–f).

To further analyse the variation characteristics of hydrological elements in different periods under future scenarios, we conducted a probability distribution curve analysis of the major hydrometeorological elements by taking positive values from a mixture of two bivariate



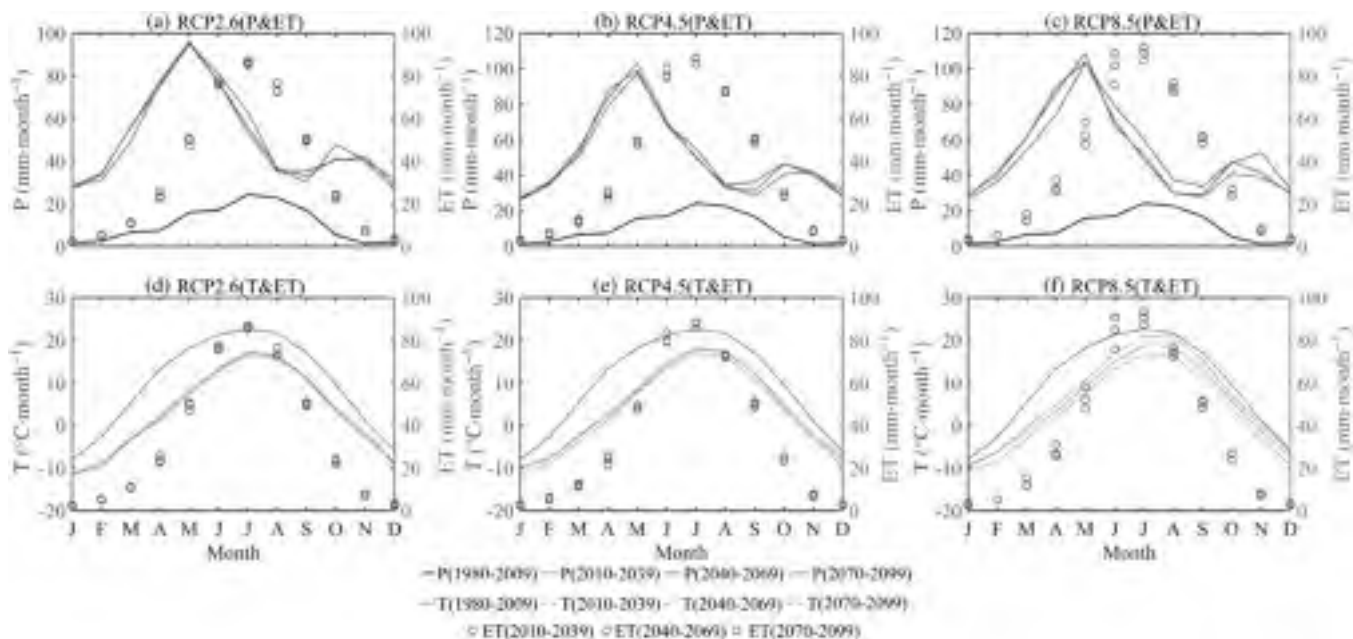


FIGURE 6 Comparison of major meteorological factors (i.e., P and T) and ETa in different months and periods in the Aksu River basin

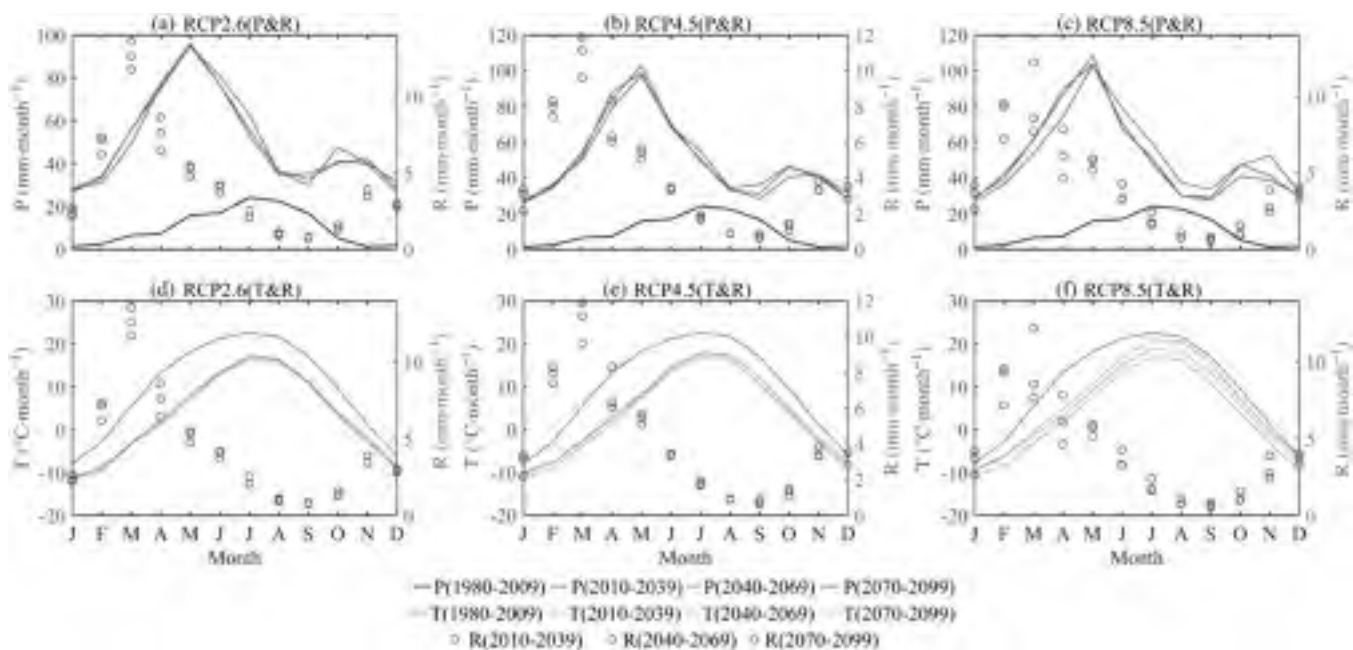


FIGURE 7 Comparison of major meteorological factors (i.e., P and T) and R in different periods and months in the Aksu River basin

normal distributions and plotting the estimated density with reflection boundary correction (Figure 9). The expectation of the probability distribution of historical precipitation was less than 0, whereas those of precipitation in the future were greater than 0. In addition, the steepness of the normal distribution of precipitation in the future was higher than that of historical precipitation.

Thus, this phenomenon indicated that precipitation in the future was significantly richer than historical precipitation. In addition, this implied that the future precipitation variability was less than that of historical precipitation. The probability distribution of historical temperature was more consistent with that of the period 2070–2099 under RCP2.6, while the variation of



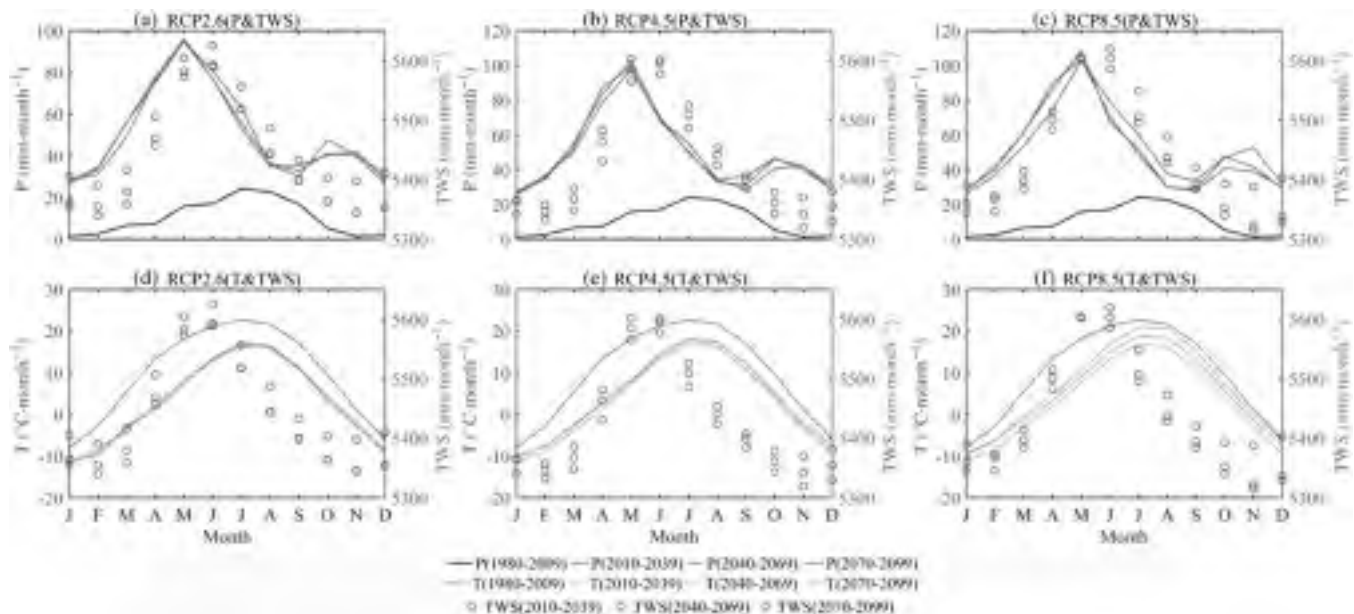


FIGURE 8 Comparison of major meteorological factors (i.e., P and T) and TWS in different months and periods in the Aksu River basin

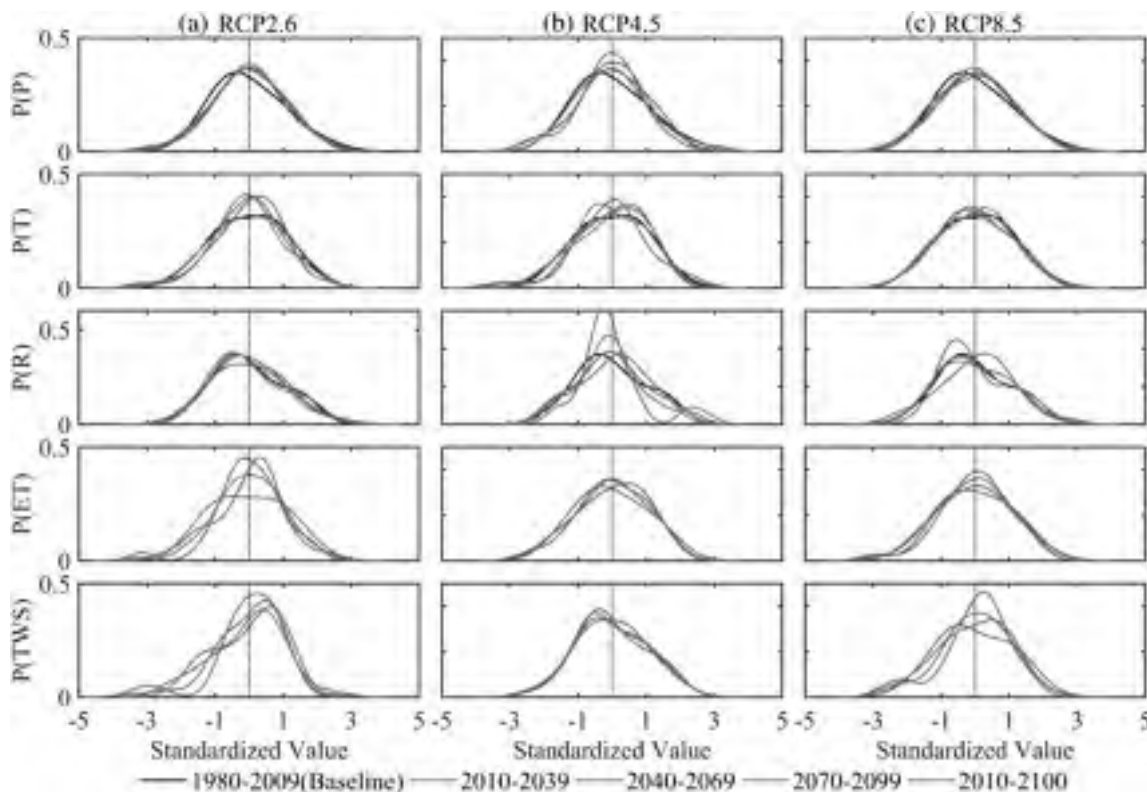


FIGURE 9 Probability density distribution of major hydrometeorological elements (i.e., P, T, ET, R, and TWS) in the Aksu River basin in different periods

temperature in other periods under RCP2.6 was smaller than that of the historical period. Meanwhile, there was an obvious difference between the mean and variance of

future temperature under RCP4.5 and those in history, while future temperature under RCP8.5 somewhat agreed with historical temperatures. Furthermore, the

expected and variance values of runoff under RCP2.6 were consistent with historical runoff, but those under RCP4.5 and RCP8.5 were not. For  $ET_a$ , there were large differences among the different periods under RCP2.6, with the standard deviation of  $ET_a$  for the period 2070–2099 being larger than those of the other three periods (i.e., 2010–2039, 2040–2069, and 2020–2100). Furthermore, the expected values and standard deviations of TWS for each period showed significant differences under RCP4.5, whereas those under RCP2.6 and RCP8.5 showed no significant differences.

### 4.3 | Influence of major meteorological factors on major hydrological elements under climate change

To further investigate the influence of major meteorological elements (i.e., precipitation and temperature) on runoff, we used the multiple wavelet coherence method (Figures 10 and 11). Figure 10 presents the multivariate wavelet analysis of the major meteorological elements (i.e., precipitation and temperature) and runoff in history. There was a very significant correlation between runoff and precipitation/temperature in the mountain region (i.e., Shaliguilanke and Xiehela). In particular, the correlation between runoff and precipitation/temperature at the Shaliguilanke hydrological station reached more than 0.9 on a 1-year time scale centred on the years 1986 and 2003, and more than 0.8 on a 5-year time scale around 1995 (Figure 10a). Precipitation and temperature were substantially associated with runoff at the Xiehela hydrological station on 3-year and 8-year periods centred on

1995, with correlations of 0.9 or higher (Figure 10b). However, in the case of the Alaer hydrological station, the correlation between runoff and precipitation/temperature was not significant (Figure 10c).

Figure 11 shows the multivariate wavelet analysis of the major meteorological elements and major hydrological factors (i.e., evapotranspiration, runoff, and TWS) under future scenarios. Both precipitation and temperature in the ARB under RCP2.6 significantly affected the major hydrological factors (i.e.,  $ET_a$ , runoff, and TWS). Among them, precipitation and temperature were significantly correlated with  $ET_a$  and runoff on a time scale of 4 and 8 years centred on 2055, with correlation coefficients above 0.9 (Figure 11a,d). In contrast, precipitation and temperature were significantly correlated with TWS over periods greater than the 4-year time scale, with correlation coefficients greater than 0.9 for 2010–2100 (Figure 11g). Under RCP4.5, the correlation between precipitation and temperature on  $ET_a$ , runoff, and TWS became more significant, especially on the 4–8-year time scale, where the correlation coefficient was greater than 0.8 (Figure 11b,e,h). TWS was more strongly linked with precipitation and temperature than  $ET_a$  and runoff (Figure 11h). However, under RCP8.5, precipitation and temperature were significantly correlated with  $ET_a$  on a 1-year time scale centred at 2070 and on a 4–8-year time scale centred at 2020 and 2080 (Figure 11c). The runoff and TWS under RCP8.5 were highly significantly correlated with precipitation and temperature on a 2–7-year time scale centred on 2030 and 2070, exceeding 0.9 (Figure 11f–l). Therefore, in general, precipitation and temperature significantly influence the major hydrological elements in the future.

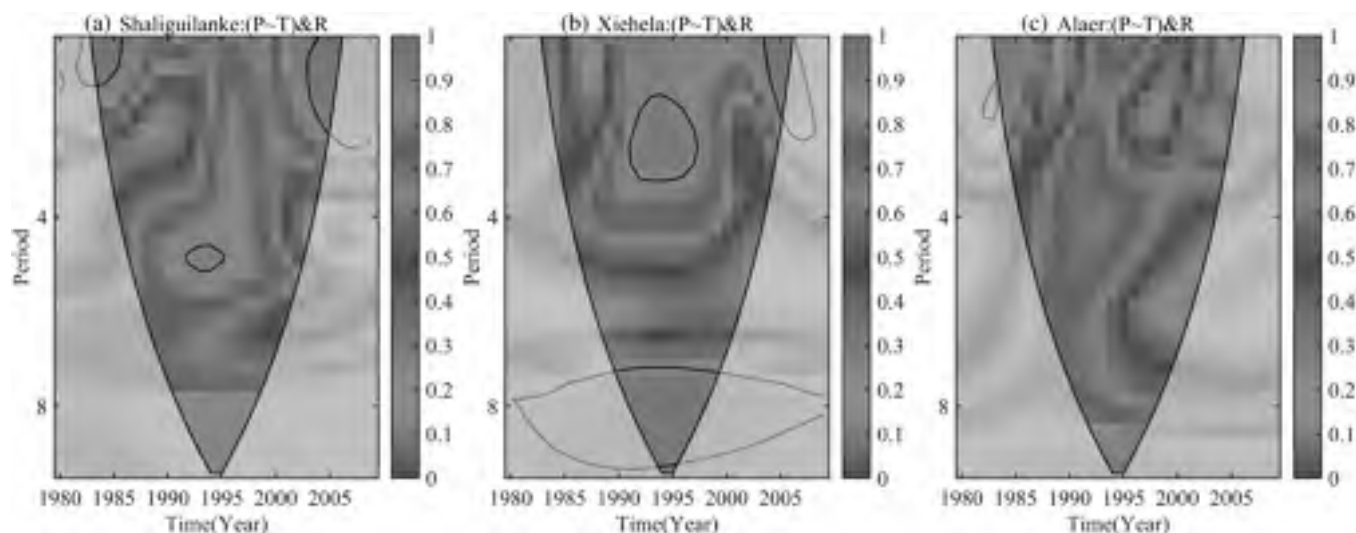


FIGURE 10 Influence of major meteorological factors on runoff in the Aksu River basin during 1980–2010

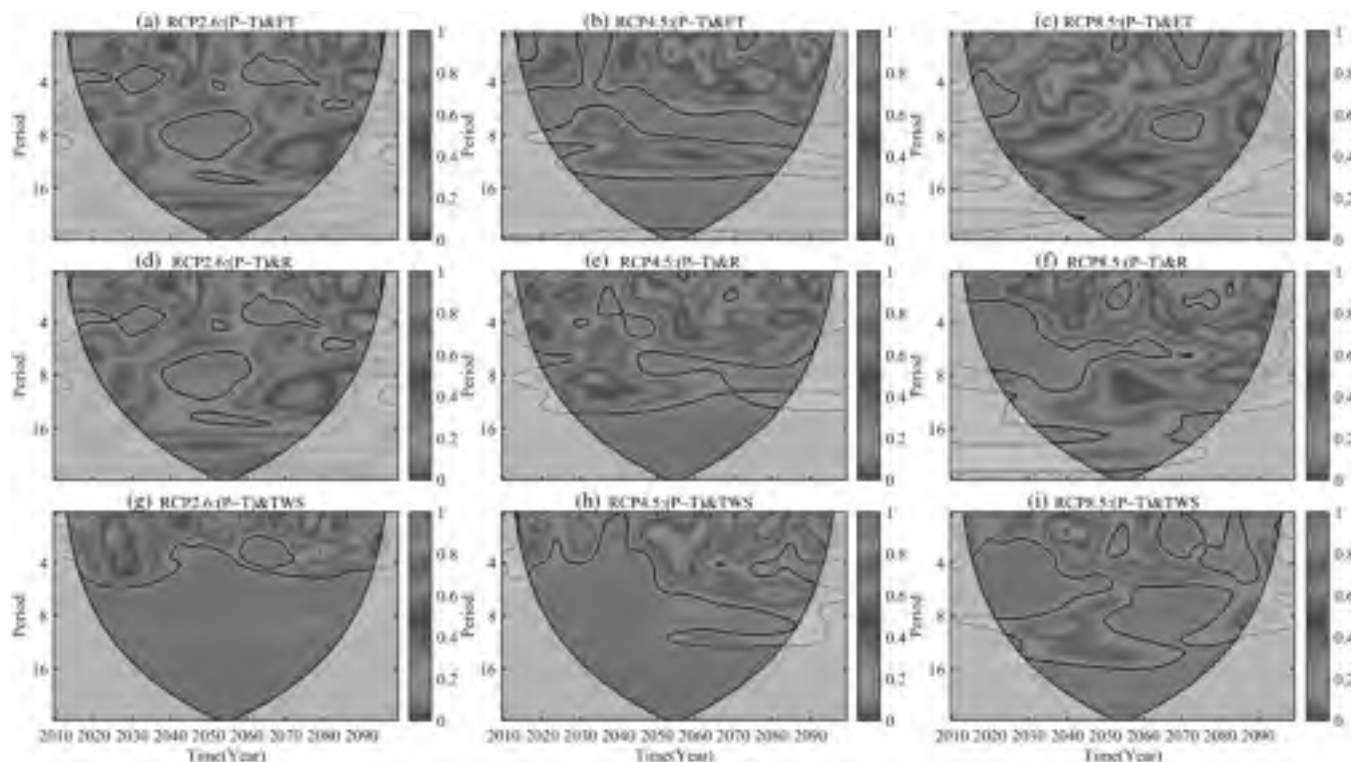


FIGURE 11 Influence of major meteorological factors on runoff in the Aksu River basin during 2010–2100

## 5 | DISCUSSION

Climate change, which has a profound impact on the safety of human life and property in natural ecosystems, has become a global concern and an urgent problem to be solved (Chen *et al.*, 2016a, 2016b). The hydrological cycle in the ARB originates from the Tianshan Mountains, which are mainly recharged by snow and ice meltwater and thus are seriously affected by climate change (Kriegel *et al.*, 2013; Wang *et al.*, 2021). The involvement of glacial and snowpack change processes in the Tianshan Mountains complicates the hydrological processes in the ARB (Chen *et al.*, 2016a; Zhang *et al.*, 2019), which can also be seen from the multivariate wavelet analysis in this study. Moreover, previous studies have shown that against the background of global warming by 0.7°C in the last 100 years, the temperature on the Tianshan Mountains has been increasing at a rate of 0.34°C per decade for the last 50 years, thereby affecting the energy and mass balance of glacier surfaces and altering the recharge of runoff and water resources (Jiang *et al.*, 2013; Ji *et al.*, 2014; Chen *et al.*, 2016a). They all demonstrated the similar findings of our study. Meanwhile, a decreasing trend in snow and ice resources and an increasing trend in runoff in the ARB have been reported in previous studies (i.e., Duethmann *et al.*, 2015),

which are also highly consistent with our findings (Figures 2 and 3). Although the future temperatures determined in this study were relatively lower than those in 1980–2009, Su *et al.* (2017) and Tao *et al.* (2014) found that future temperatures are significantly higher than those in 1960–2010, which would have important implications for snow and ice resources and runoff in the ARB.

The increased precipitation and significant wetting in the Tarim Basin over the past decades under the influence of teleconnection indices would also impact the runoff in the ARB in the future (Tao *et al.*, 2014; Wang *et al.*, 2014). These results are highly consistent with our study, especially the runoff from the Shaliguilanke and Xiehela hydrological stations. However, runoff in the Alaer hydrological station was not significantly correlated with precipitation and temperature (e.g., Figure 10). According to previous studies, the reason for this is the development of irrigated agriculture in the ARB, where the arable land and population have increased, along with water demand for agricultural irrigation (Tao *et al.*, 2011; Yang *et al.*, 2018a; 2018b; Yang *et al.*, 2021). Consequently, runoff in the Alaer hydrological station did not increase due to a rise in runoff from the mountains (Huang *et al.*, 2015; Yang *et al.*, 2021), which explains our findings well.

In addition,  $ET_a$  is an important component of the water cycle, which also changes significantly under



climate change (Su *et al.*, 2017; Yang *et al.*, 2018a; 2018b). Yang *et al.* (2018a) reported that  $ET_a$  and agricultural water consumption in the ARB have increased significantly in the past two decades based on the Vegetation Interfaces Processes model; they also quantified climate change as the major factor influencing  $ET_a$  in the ARB. Su *et al.* (2017) found that  $ET_a$  in the TRB averaged 222.7 mm for global warming of 1.5°C (2020–2039), which is 6.9 mm higher than that in the baseline period from 1986 to 2005. Therefore, the findings of this study regarding the close relationship between changes in  $ET_a$  and climate change are consistent with those of previous studies.

Moreover, TWS is an essential part of the coupled relationship between global climate change and the water cycle (Yang and Chen, 2015; Chen *et al.*, 2016a; Deng *et al.*, 2019). Our results showed that TWS on the southern slopes of the Tianshan Mountains in central Asia is on a declining trend, which is very similar to the findings of Yang and Chen (2015) and Deng *et al.* (2019); this could have important implications for runoff recharge in the middle and lower reaches of the river. Moreover, Chen *et al.* (2016a) pointed out that the changes in TWS in the Tianshan Mountains are closely related to the distribution of glaciers/snow cover and the variation in temperature and precipitation, which corroborates the results of the multivariate wavelet analysis. If the climate continues to change, the glaciers, snow cover, and TWS will continue to decrease, resulting in an inevitable shortening and drying of some rivers in the ARB in the next few decades (Barnett *et al.*, 2005; Chen *et al.*, 2016a). Overall, this study is a good predictor of the variability of the main hydrological elements in the ARB by explaining the effect of climate change on the hydrological elements, which are of great importance for guiding the development of irrigated agriculture and rational exploitation of water resources in the ARB.

## 6 | CONCLUSION

In this study, the hydrological processes in the ARB in historical and future scenarios were simulated using CLM-DTVGM and CMIP5 data, and the impact of climate change on the major hydrological processes in the ARB in different future periods (i.e., 1980–2009, 2010–2039, 2040–2069, 2070–2099, and 2010–2100) were evaluated. The primary conclusions are as follows:

1. As the determination coefficient and Nash–Sutcliffe efficiency coefficient reached desirable levels, CLM-DTVGM afforded a better simulation of runoff in the ARB; runoff in the future scenario was found to be

shallower in the irrigation area, where the decreasing trend of runoff was much more significant than in other regions.

2. Accompanied by changes in precipitation and temperature in the baseline year, runoff,  $ET_a$ , and TWS in the future scenario changed significantly; specifically, runoff and TWS decreased, whereas  $ET_a$  increased.
3. Historically, runoff from Shaliguilanke and Xiehela was significantly affected by climate change, with correlation coefficients exceeding 0.9; however, runoff from the Alaer station was not significantly affected by climate change. Runoff,  $ET_a$ , and TWS in the ARB were closely correlated with climate change in future scenarios. Related research is important in guiding the sustainable development of arid regions in north-west China. Except for the important influence of climate change, human activities also have a significant impact on hydrological processes, so the integrated consideration of the influence of human activities and climate change on hydrological processes is an important theme of our research in the future.

## ACKNOWLEDGEMENTS

We would like to express our sincere thanks to all data supporters and websites. Meanwhile, the research is supported by the Foundation: Youth Fund for Humanities and Social Science Research of the Ministry of Education (No. 20YJCZH207) and Strategic Priority Research Program of the Chinese Academy of Sciences (No. XDA23040504).

## AUTHOR CONTRIBUTIONS

**Peng Yang:** Writing – original draft. **Wenyu Wang:** Software; visualization. **Jun Xia:** Supervision. **Yaning Chen:** Supervision. **Chesheng Zhan:** Methodology. **Shengqing Zhang:** Data curation. **Cai Wei:** Methodology. **Xiangang Luo:** Software. **Jiang Li:** Investigation.

## ORCID

Peng Yang  <https://orcid.org/0000-0002-6311-3083>

Cai Wei  <https://orcid.org/0000-0003-2054-5174>

## REFERENCES

- Barnett, T.P., Adam, J.C. and Lettenmaier, D.P. (2005) Potential impacts of a warming climate on water availability in snow-dominated regions. *Nature*, 438, 303–309.
- Bronselaer, B., Winton, M., Griffies, S.M., Hurlin, W.J., Rodgers, K. B., Sergienko, O.V., Stouffer, R.J. and Russell, J.L. (2018) Change in future climate due to Antarctic meltwater. *Nature*, 564, 53–58.
- Chang, E., Guo, Y.J. and Xia, X. (2012) CMIP5 multimodal ensemble projection of storm track change under global warming. *Journal of Geophysical Research*, 117(D23), 1–19. <https://doi.org/10.1029/2012JD018578>.



- Chen, G., Li, X., Liu, X., Chen, Y., Liang, X., Leng, J., Xu, X., Liao, W., Wu, Q. and Huang, K. (2020) Global projections of future urban land expansion under shared socioeconomic pathways. *Nature Communications*, 11(1), 1–12.
- Chen, Y.N., Deng, H.J., Li, B.F., Li, Z. and Xu, C.C. (2014) Abrupt change of temperature and precipitation extremes in the arid region of northwest China. *Quaternary International*, 336(12), 35–43.
- Chen, Y.N., Li, W.H., Deng, H.J., Fang, G.H. and Li, Z. (2016b) Changes in central Asia's water tower: past, present and future. *Scientific Reports*, 6, 39364.
- Chen, Y.N., Li, Z., Li, W.H., Deng, H.J. and Shen, Y.J. (2016a) Water and ecological security: dealing with hydroclimatic challenges at the heart of China's Silk Road. *Environment and Earth Science*, 75, 881.
- Chen, Y.N., Xu, C.C., Hao, X.M., Li, W.H. and Chen, Y.P. (2009) Fifty-year climate change and its effect on annual runoff in the Tarim River basin, China. *Quaternary International*, 208, 53–61.
- Conway, D. and Schipper, E.L. (2011) Adaptation to climate change in Africa: challenges and opportunities identified from Ethiopia. *Global Environmental Change*, 21, 227–237.
- Dai, A., Rasmussen, R.M., Ikeda, K. and Liu, C. (2020) A new approach to construct representative future forcing data for dynamic downscaling. *Climate Dynamics*, 55(1–2), 1–9.
- Deng, H., Chen, Y. and Yang, L. (2019) Glacier and snow variations and their impacts on regional water resources in mountains. *Journal of Geographical Sciences*, 29(1), 84–100.
- Duethmann, D., Bolch, T., Farinotti, D., Kriegel, D., Vorogushyn, S., Merz, B., Pieczonka, T., Jiang, T., Su, B. and Güntner, A. (2015) Attribution of streamflow trends in snow and glacier melt-dominated catchments of the Tarim River, central Asia. *Water Resources Research*, 51(6), 4727–4750.
- Fan, Y., Chen, Y.N. and Li, W.H. (2014) Increasing precipitation and baseflow in Aksu River since the 1950s. *Quaternary International*, 336, 26–34.
- Fu, G., Liu, Z., Charles, S.P., Xu, Z. and Yao, Z. (2013) A score-based method for assessing the performance of GCMs: a case study of southeastern Australia. *Journal of Geophysical Research*, 118, 4154–4167.
- Grinsted, A., Moore, J.C. and Jevrejeva, S. (2004) Application of the cross wavelet transform and wavelet coherence to geophysical time series. *Nonlinear Processes in Geophysics*, 11(5/6), 561–566.
- Gudmundsson, L., Boulange, J., Hong, X.D., Gosling, S.N., Grillakis, M.G., Koutroulis, A.G., Leonard, M., Liu, J., Schmied, H.M. and Zhao, F. (2021) Globally observed trends in mean and extreme river flow attributed to climate change. *Science*, 371, 1159–1162. <https://doi.org/10.1126/science.aba3996>.
- Homsí, R. (2020) Precipitation projection using a CMIP5 GCM ensemble model: a regional investigation of Syria. *Engineering Applications of Computational Fluid*, 14(1), 90–106.
- Hu, J.Y., Wu, Y.P., Sun, P.C., Zhao, F.B., Sun, K., Li, T.J., Sivakumare, B., Qiu, L.J., Sun, Y.Z. and Jin, Z.D. (2021) Predicting long-term hydrological change caused by climate shifting in the 21st century in the headwater area of the Yellow River basin. *Stochastic Environmental Research and Risk Assessment*, 18, 1–18. <https://doi.org/10.1007/s00477-021-02099-6>.
- Hu, W. and Si, B.C. (2016) Multiple wavelet coherence for untangling scale-specific and localized multivariate relationships in geosciences. *Hydrology and Earth System Sciences*, 20(8), 3183–3191.
- Huang, S., Krysanova, V., Zhai, J. and Su, B.D. (2015) Impact of intensive irrigation activities on river discharge under agricultural scenarios in the semi-arid Aksu River basin, northwest China. *Water Resources Management*, 29(3), 945–959.
- Huntington, T.G. (2006) Evidence for intensification of the global water cycle: review and synthesis. *Journal of Hydrology*, 319, 83–95.
- Ji, F., Wu, Z.H., Huang, J.P. and Chassignet, E.P. (2014) Evolution of land surface air temperature trend. *Nature Climate Change*, 4, 462–466.
- Jiang, Y.A., Chen, Y., Ye, Z.X., Chen, Y.P., Yu, X.J., Fan, J. and Bai, S.Q. (2013) Analysis on changes of basic climatic elements and extreme events in Xinjiang, China during 1961–2010. *Advances in Climate Change Research*, 4(1), 20–29.
- Koven, C.D., Riley, W.J. and Stern, A. (2013) Analysis of permafrost thermal dynamics and response to climate change in the CMIP5 Earth System Models. *Journal of Climate*, 26(6), 1877–1900.
- Kriegel, D., Mayer, C., Hagg, W., Vorogushyn, S., Duethmann, D., Gafurov, A. and Farinotti, D. (2013) Changes in glacier station, climate and runoff in the second half of the 20th century in the Naryn basin, central Asia. *Global and Planetary Change*, 110, 51–61.
- Li, L., Xia, J., Xu, C.Y., Chu, J.J., and Wang, R. (2009) Analyse the sources of equifinality in hydrological model using GLUE methodology. Paper presented at Hydroinformatics in Hydrology, Hydrogeology & Water Resources Proceedings of Symposium Js4 at the Joint Iahs & Iah Convention, Hyderabad, India, September, 2009.
- Mastrotheodoros, T., Pappas, C., Molnar, P., Burlando, P., Manoli, G., Parajka, J., Rigon, R., Szele, B., Bottazzi, M., Hadjidoukas, P. and Faticchi, S. (2020) More green and less blue water in the Alps during warmer summers. *Nature Climate Change*, 10, 155–161.
- Mcsweeney, C.F., Jones, R.G., Lee, R.W. and Rowell, D.P. (2015) Selecting CMIP5 GCMs for downscaling over multiple regions. *Climate Dynamics*, 44(11–12), 3237–3260.
- Meaurio, M., Zabaleta, A., Boithias, L., Epelde, A.M., Sauvage, S., Sánchez-Pérez, J.M., Srinivasan, R. and Antigüedad, I. (2017) Assessing the hydrological response from an ensemble of CMIP5 climate projections in the transition zone of the Atlantic region (Bay of Biscay). *Journal of Hydrology*, 1, 46–62.
- Mengistu, D., Bewket, W., Dosio, A. and Panitz, H.J. (2021) Climate change impacts on water resources in the Upper Blue Nile (Abay) River basin, Ethiopia. *Journal of Hydrology*, 592, 125614.
- Niu, G.Y. and Yang, Z.L. (2006) Effects of frozen soil on snowmelt runoff and soil water storage at a continental scale. *Journal of Hydrometeorology*, 7, 937–952.
- Pokhrel, Y., Felfelani, F., Satoh, Y., Boulange, J., Burek, P., Gädeke, A., Gerten, D., Gosling, S.N., Grillakis, M., Gudmundsson, L., Hanasaki, N., Kim, H., Koutroulis, A., Liu, J.G., Papadimitriou, L., Schewe, J., Schmied, H.M., Stacke, T., Telteu, C.E., Thiery, W., Veldkamp, T., Zhao, F. and Wada, Y. (2021) Global terrestrial water storage and drought severity under climate change. *Nature Climate Change*, 11(3), 226–233.
- Qin, Y., Abatzoglou, J.T., Siebert, S., Huning, L.S., AghaKouchak, A., Mankin, J.S., Hong, C.P., Tong, D., Davis, S. J. and Mueller, N.D. (2020) Agricultural risks from changing snowmelt. *Nature Climate Change*, 10, 459–465.
- Song, X.M., Zhan, C.S., Kong, F.Z. and Xia, J. (2011) Advances in the study of uncertainty quantification of large-scale hydrological modeling system. *Journal of Geographical Sciences*, 21(5), 801–819.

- Su, B., Jian, D., Li, X., Wang, Y.J., Wang, A.Q., Wen, S.S., Tao, H. and Hartmann, H.K. (2017) Projection of actual evapotranspiration using the COSMO-CLM regional climate model under global warming scenarios of 1.5°C and 2.0°C in the Tarim River basin, China. *Atmospheric Research*, 196, 119–128.
- Su, L., Miao, C., Duan, Q.Y., Lei, X. and Li, H. (2019) Multiple-wavelet coherence of world's large rivers with meteorological factors and ocean signals. *Journal of Geophysical Research*, 124, 4932–4954. <https://doi.org/10.1029/2018JD029842>.
- Tao, H., Borth, H., Fraedrich, K., Su, B.D. and Zhu, X.H. (2014) Drought and wetness variability in the Tarim River basin and connection to large-scale atmospheric circulation. *International Journal of Climatology*, 34(8), 2678–2684.
- Tao, H., Gemmer, M., Bai, Y., Su, B.D. and Mao, W. (2011) Trends of streamflow in the Tarim River basin during the past 50 years: human impact or climate change? *Journal of Hydrology*, 400(1–2), 1–9.
- Thornton, P.E. and Zimmermann, N.E. (2007) An improved canopy integration scheme for a land surface model with prognostic canopy structure. *Journal of Climate*, 20, 3902–3923.
- Tian, B. and Dong, X. (2020) The double-ITCZ bias in CMIP3, CMIP5, and CMIP6 models based on annual mean precipitation. *Geophysical Research Letters*, 47(8), e2020GL087232.
- Wang, C., Xu, J., Chen, Y., Bai, L. and Chen, L. (2018) A hybrid model to assess the impact of climate variability on streamflow for an ungauged mountainous basin. *Climate Dynamics*, 50(7–8), 2829–2844. <https://doi.org/10.1007/s00382-017-3775-x>.
- Wang, H., Chen, Y.N. and Li, W.H. (2014) Hydrological extreme variability in the headwater of Tarim River: links with atmospheric teleconnection and regional climate. *Stochastic Environmental Research and Risk Assessment*, 28(2), 443–453.
- Wang, M. (2012) A sea ice free summer Arctic within 30 years: an update from CMIP5 models. *Geophysical Research Letters*, 39, L18501.
- Wang, X.X., Chen, Y.N., Li, Z., Fang, G.H. and Hao, H.C. (2021) Water resources management and dynamic changes in water politics in the transboundary river basins of Central Asia. *Hydrology and Earth System Sciences*, 25(6), 3281–3299.
- Xia, J. (2002) *Hydrological Nonlinear System Theory and Method*. Wuhan: Wuhan University Press, pp. 369–400 (in Chinese).
- Xia, J., Luo, Y., Duan, Q.Y., Mo, X.G., Liu, Z.Y. and Xie, Z.H. (2016) *Impacts of Climate Change on Land Water Cycle and Water Resources Security in the Monsoon Region of Eastern China and Adaptation Countermeasures*. Beijing: Science Press, pp. 154–200 (in Chinese).
- Xu, J.H., Chen, Y.N., Lu, F. and Li, W.H. (2011) The nonlinear trend of runoff and its response to climate change in the Aksu River, western China. *International Journal of Climatology*, 31(5), 687–695.
- Yang, P. and Chen, Y.N. (2015) An analysis of terrestrial water storage variations from GRACE and GLDAS: the Tianshan Mountains and its adjacent areas, central Asia. *Quaternary International*, 358, 106–112.
- Yang, P., Xia, J., Zhan, C.S., Chen, X.J. and Qiao, Y.F. (2018b) Separating the impacts of climate change and human activities on actual evapotranspiration of multi-ecosystems in the Aksu River basin, northwest China. *Hydrology Research*, 136, 1740–1752.
- Yang, P., Xia, J., Zhan, C.S., Mo, X.G., Chen, X.J., Hu, S. and Chen, J. (2018a) Estimation of water consumption for ecosystems based on vegetation interfaces processes model: a case study of the Aksu River basin, northwest China. *Science of the Total Environment*, 613–614, 186–195.
- Yang, P., Xia, J., Zhang, Y.Y. and Hong, S. (2017) Temporal and spatial variations of precipitation in northwest China during 1960–2013. *Atmospheric Research*, 183, 283–295.
- Yang, P., Xia, J., Zhang, Y.Y., Zhan, C.S. and Sun, S.X. (2019a) How is the risk of hydrological drought in the Tarim River basin, northwest China? *Science of the Total Environment*, 693, 13355.
- Yang, P., Xia, J.Y., Zhang, Y.Y., Zhan, C.S., Cai, W., Zhang, S.Q. and Wang, W.Y. (2021) Quantitative study on characteristics of hydrological drought in arid area of northwest China under changing environment. *Journal of Hydrology*, 597(25), 126343.
- Yang, Y.T., Michael, R. and Zhang, S.L. (2019b) Hydrologic implications of vegetation response to elevated CO<sub>2</sub> in climate projections. *Nature Climate Change*, 9, 44–48.
- Yao, J., Chen, Y., Zhao, Y., Guan, X.F., Mao, W.Y. and Yang, L.M. (2020) Climatic and associated atmospheric water cycle changes over the Xinjiang, China. *Journal of Hydrology*, 585, 124823.
- Yin, J., Guo, S., Gentile, P., Sullivan, S.C. and Liu, P. (2021) Does the Hook structure constrain future flood intensification under anthropogenic climate warming? *Water Resources Research*, 57(2), e2020WR028491.
- Zhan, C.S., Song, X.M. and Xia, J. (2013) An efficient integrated approach for global sensitivity analysis of hydrological model parameters. *Environmental Modelling and Software*, 41, 39–52.
- Zhang, Q.F., Chen, Y.N., Li, Z., Li, Y.P., Xiang, Y. and Bian, W. (2019) Glacier changes from 1975 to 2016 in the Aksu River basin, central Tianshan Mountains. *Journal of Geographical Sciences*, 29(006), 984–1000.
- Zhang, Y.Y., Fu, G.B., Sun, B.Y., Zhang, S.F. and Men, B.H. (2015) Simulation and classification of the impacts of projected climate change on flow regimes in the arid Hexi Corridor of northwest China. *Journal of Geophysical Research*, 120(15), 7429–7453.
- Zhao, F., Wu, Y., Yao, Y., Sun, K. and Sun, Y. (2019) Predicting the climate change impacts on water-carbon coupling cycles for a loess Hilly-gully watershed. *Journal of Hydrology*, 581, 124388.

**How to cite this article:** Yang, P., Wang, W., Xia, J., Chen, Y., Zhan, C., Zhang, S., Wei, C., Luo, X., & Li, J. (2022). Effects of climate change on major elements of the hydrological cycle in Aksu River basin, northwest China. *International Journal of Climatology*, 42(10), 5359–5372. <https://doi.org/10.1002/joc.7537>